Journal of Medicinal Chemistry

Article

pubs.acs.org/jmc

A Potent Small-Molecule Inhibitor of the MDM2−p53 Interaction (MI-888) Achieved Complete and Durable Tumor Regression in Mice

Yujun Zhao,[†,§] Shanghai Yu,[†,§] Wei Sun,[†,§] Liu Liu,[†] Jianfeng Lu,[†] Donna McEachern,[†] Sanjeev Shargary,[†] Denzil Bernard,[†] Xiaoqin Li,[‡] Ting Zhao,[‡] Peng Zou,[‡] Duxin Sun,[‡] and Shaomeng Wang*[,†]

[†]Comprehensive Cancer Center and Departments of Internal Medicine, Pharmacology, and Medicinal Chemistry, University of Michigan, Ann Arbor, Michigan 48109, United States

[‡]Department of Pharmaceutical Sciences, College of Pharmacy, University of Michigan, Ann Arbor, Michigan 48109, United States

ABSTRACT: We previously reported the discovery of a class of spirooxindoles as potent and selective small-molecule inhibitors of the MDM2−p53 interaction (MDM2 inhibitors). We report herein our efforts to improve their pharmacokinetic properties and in vivo antitumor activity. Our efforts led to the identification of **9** (MI-888) as a potent MDM2 inhibitor (K_i = 0.44 nM) with a superior pharmacokinetic profile and enhanced in vivo efficacy. Compound **9** is capable of achieving rapid, complete, and durable tumor regression in two types of xenograft models of human cancer with oral administration and represents the most potent and efficacious MDM2 inhibitor reported to date.

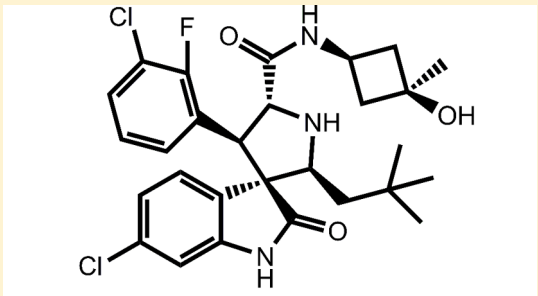

Compound **9**, A Potent MDM2 Inhibitor Capable of Achieving Complete Tumor Regression

INTRODUCTION

Tumor suppressor protein p53 is a transcription factor and plays a key role in regulation of cell cycle, apoptosis, DNA repair, senescence, and angiogenesis, among other cellular processes.[1−3] In approximately half of human cancers, *TP53*, the gene encoding p53 protein, is deleted or mutated, which renders loss of the tumor suppressor function of p53.[4] In the other half of human cancers, p53 retains wild-type status but its tumor suppressor function is effectively inhibited by its primary endogenous inhibitor, the murine double minute 2 protein (MDM2, or HDM2 in humans).[5] MDM2 inhibits the function of p53 by multiple mechanisms, but all are mediated by their direct protein−protein interaction.[5] The cocrystal structure of MDM2 in complex with p53 has shown that their binding involves primarily three key residues in p53 (Phe19, Trp23, and Leu26) and a well-defined, surface binding pocket in MDM2,[6] suggesting the possibility of designing non-peptide, small-molecule inhibitors to block the MDM2−p53 protein−protein interaction (hereafter called MDM2 inhibitors). Such small-molecule inhibitors may have a promising therapeutic potential for the treatment of human cancer by reactivation of the powerful tumor suppressor function of p53.[7−10] Vassilev and his colleagues from Hoffmann-La Roche were the first to report potent, selective, and orally bioavailable, small-molecule MDM2 inhibitors, as exemplified by nutlin-3.[7] In the past few years, there has been intense research interest in the design of new small-molecule MDM2 inhibitors, from both academia and industry.[8,11−21]

Our group has previously reported structure-based design of a series of spirooxindoles as a new class of potent and selective MDM2 inhibitors.[8,11−13,21] Two of such compounds, **1** (MI-219)[8] and **2**[21] (Figure 1) bind to MDM2 with low nanomolar affinities (Table 1) and are orally active in preclinical animal models of human cancer. While both compounds inhibited tumor growth in the SJSA-1 xenograft model in mice, high oral doses (200−300 mg/kg) were needed. Furthermore, these MDM2 inhibitors failed to achieve complete tumor regression.[8,21] Collectively, these data suggest that the pharmacokinetics (PK) properties and in vivo efficacy for **1** and **2** need to be further improved for clinical development.

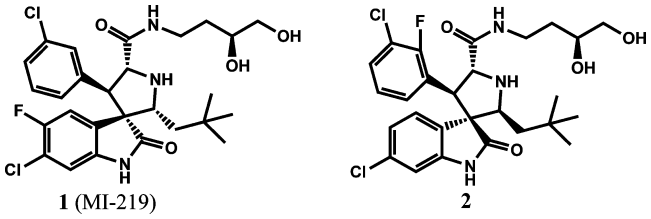

1 (MI-219) **2**

Figure 1. Two of our previously reported potent and orally active MDM2 inhibitors.

Since **2** has a higher binding affinity to MDM2 and more potent cellular activity in cancer cells than **1**,[21] we have focused our modifications on **2** with the goal of improving its PK properties and in vivo antitumor activity. Our efforts have now yielded a highly potent MDM2 inhibitor **9** (MI-888)[21] with improved oral PK properties and in vivo antitumor activity. In fact, **9** was capable of achieving complete and long-lasting

Received: April 18, 2013
Published: June 20, 2013

Table 1. MDM2 Binding Affinity and Cell Growth Inhibition Data for 1−10

compd	binding IC_{50} (nM)	K_i (nM)	IC_{50} (μM) SJSA-1 cell line	IC_{50} (μM) RS4;11 cell line
1	44.6 ± 2.7	10.5 ± 2.0	0.89 ± 0.21	0.54 ± 0.14
2	9.8 ± 2.7	0.86 ± 0.11	0.25 ± 0.04	0.10 ± 0.01
3	7.1 ± 1.5	0.61 ± 0.10	0.24 ± 0.05	0.12 ± 0.01
4	8.2 ± 2.3	1.1 ± 0.3	0.41 ± 0.04	0.30 ± 0.06
5	8.8 ± 1.4	0.94 ± 0.07	0.32 ± 0.06	0.23 ± 0.04
6	8.4 ± 1.1	0.62 ± 0.05	0.20 ± 0.02	0.10 ± 0.02
7	16.3 ± 2.1	2.4 ± 0.5	0.35 ± 0.06	0.21 ± 0.05
8	11.1 ± 2.1	0.97 ± 0.3	0.60 ± 0.16	0.43 ± 0.07
9	6.8 ± 0.9	0.44 ± 0.22	0.08 ± 0.02	0.06 ± 0.01
10	7.6 ± 0.9	0.62 ± 0.19	0.25 ± 0.04	0.10 ± 0.01

tumor regression in animal models of human cancer upon oral administration.

RESULTS AND DISCUSSION

Both **1** and **2** have a flexible 1,2-diol side chain, which was shown to enhance their binding affinities to MDM2 by several times and to play a role in modulating their oral pharmacokinetics properties in our previous studies.[11,21] Our metabolic studies of **2** revealed that the major metabolic soft spots are located in the 1,2-diol side chain (data not shown). We hypothesized that the overall oral PK profile of **2** can be improved by conformationally constraining the 1,2-diol side chain, thus reducing the number of rotatable bonds in the molecule, and by further improving the metabolic stability.

Although the side chain in **1** and in **2** contains two hydroxyl groups, we retained only one hydroxyl group in **3**−**7** containing a conformationally constrained side chain for consideration of synthetic feasibility (Figure 2). Their binding affinities to MDM2 were determined using our optimized fluorescence-polarization (FP) binding assay,[21] and the results are summarized in Table 1.

The binding data showed that **3**−**6** with a cyclic alcohol side chain bind to MDM2 with high affinities (K_i = 0.61−1.1 nM). These compounds are as potent as **2** but 10 times more potent than **1**. However, **7** with a *tert*-butanol side chain is 3 times less potent than **2** in binding to MDM2.

We tested **1**−**7** for their ability to inhibit cell growth in SJSA-1 osteosarcoma and RS4;11 acute leukemia cell lines, which have wild-type p53 and are sensitive to MDM2 inhibitors. The results are summarized in Table 1. Compounds **3** and **6** have IC_{50} values of 0.24 μM in the SJSA-1 cell line and 0.12 μM in the RS4;11 cell line and are as potent as **2**. Compounds **4**, **5**, and **7** are slightly less potent than **2**, **3**, and **6** in these two cancer cell lines.

Compounds **3**−**7** were evaluated for their metabolic stability in mouse, rat, and human microsomes, in direct comparison with **1** and **2** (Table 2). In mouse microsomes, **1**, **2**, **3**, **6**, and **7**

Table 2. Stability of MDM2 Inhibitors in Mouse, Rat, and Human Microsomes

compd	$T_{1/2}$ (min) mouse microsome	rat microsome	human microsome
1	>60	20.2	>60
2	>60	16.3	>60
3	>60	19.1	54.1
4	20.6	22.1	30.8
5	1.5	3.8	4.0
6	>60	21.1	55.1
7	>60	>60	>60
8	>60	>60	>60
9	>60	>60	>60
10	>60	>60	53.3

have similar $T_{1/2}$ values ($T_{1/2}$ > 60 min) and are stable. However, **4** has modest stability ($T_{1/2}$ = 20.6 min) and **5** is very unstable ($T_{1/2}$ = 1.5 min). In rat microsomes, compounds **1**, **2**, **3**, and **6** have a shorter $T_{1/2}$ than in mouse microsomes, but **7** is quite stable ($T_{1/2}$ >60 min), whereas **5** is very unstable ($T_{1/2}$ = 3.8 min). In human microsomes, the trend is very similar to that in mouse microsomes, and **1**, **2**, **3**, **6**, and **7** have good microsomal stability.

The excellent microsomal stability for **7** in mouse, rat, and human microsomes suggested that trisubstituted-alcohol-containing side chain may block or retard the potential oxidation by cytochrome P450 enzymes. To test this hypothesis, we installed a methyl group on the hydroxyl-substituted carbon of **3** and **4**, which resulted in **8** and **9** both tethering a trisubstituted-alcohol-containing side chain. We also replaced the hydroxyl group with a methylsulfonamide group in

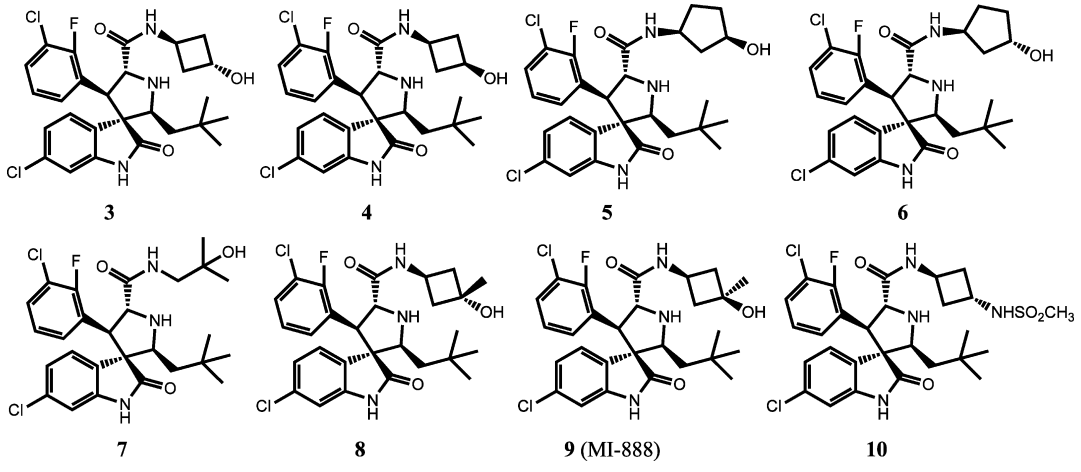

Figure 2. Chemical structures of compounds with constrained side chains.

dx.doi.org/10.1021/jm4005708 | J. Med. Chem. 2013, 56, 5553−5561

3, which yielded **10**. Microsomal stability evaluation confirmed that **8**–**10** are very stable in mouse, rat, and human microsomes (Table 2). Furthermore, our binding data (Table 1) showed that **8**–**10** have essentially the same high binding affinity to MDM2 as **2**. In the cell growth inhibition assay, **8** is 2–4 times less potent than **2**, whereas **9** is 2 times more potent than **2**, and **10** has the same potency as **2** in both cell lines (Table 1). Therefore, **9** is the most potent MDM2 inhibitor among these compounds based upon their potencies in inhibition of cell growth in these two cancer cell lines.

Upon the basis of the high binding affinity, potent cellular activity, and excellent microsomal stability, we selected **9** for evaluation of its oral PK properties in rats, in comparison to **2**. Our PK data showed that **9** has an improved PK profile in rats over **2** (Figure 3 and Table 3). The C_{max} and AUC values for **9**

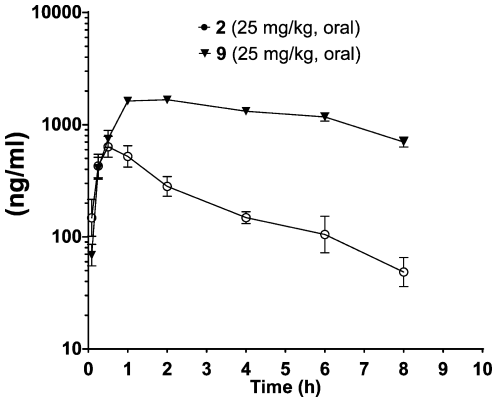

Figure 3. Oral pharmacokinetics of **2** and **9** in Sprague–Dawley rats.

Table 3. Summary of Oral Pharmacokinetic Data for 2 and 9 in Sprague–Dawley Rats

compd	dose (mg/kg)	route	C_{max} (μg/L)	AUC ($0 \rightarrow t$) (μg L^{-1} h^{-1})	$T_{1/2}$ (h)
2	25	oral	675 ± 274	2138 ± 775	3.4 ± 0.5
9	25	oral	1726 ± 100	14874 ± 2491	3.2 ± 0.5

are 2.6- and 7-fold higher than those for **2**, respectively, at the same dose, and these two compounds have a similar $T_{1/2}$ value (3.4 and 3.2 h for **2** and **9**, respectively).

Next, we examined p53 activation by **9** in the SJSA-1 osteosarcoma cell line by Western blot analysis and included **2** and nutlin-3a[7] as control compounds (Figure 4). All three compounds effectively and dose-dependently activate p53, as evidenced by the accumulation of the p53 protein, as well as MDM2 and p21, two p53 targeted gene products. In addition, treatment of three compounds dose-dependently diminished full-length poly (ADP-ribose) polymerase (PARP) at 24 h, which indicated dose-dependent apoptosis induction. Treatment of **9** activated p53 at concentrations as low as 30 nM, as evident by clear accumulation of p21 and p53. In comparison, **9** is at least 3 times more potent than **2** in p53 activation and is 10 times more potent than nutlin-3a.

Upon the basis of the molecular mechanism of action, the cellular activity of a specific MDM2 inhibitor should be dependent upon the activation of wild-type p53. To firmly assess the cellular specificity of **9**, we employed the HCT-116 p53$^{+/+}$ colon cell line and its isogenic p53 knockout (HCT-116 p53$^{-/-}$) cell line. Compound **9** potently inhibited cell growth in the HCT-116 p53$^{+/+}$ colon cell line with an IC_{50} of 92 nM and

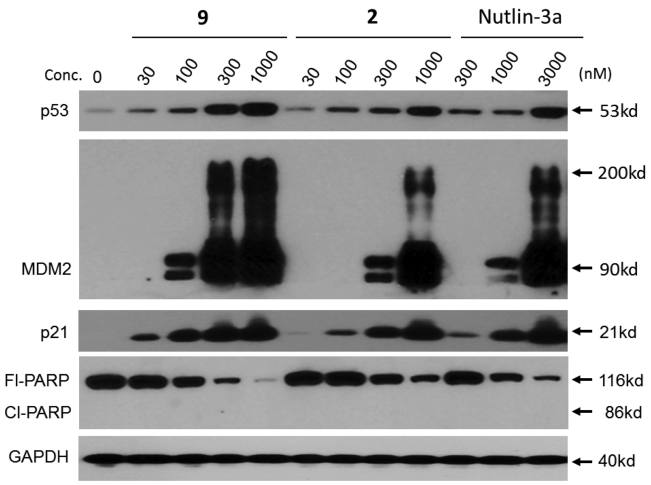

Figure 4. Western blot analysis of p53 activation and PARP cleavage in the SJSA-1 cancer cell line by **2**, **9**, and nutlin-3a. Cells were treated with different concentrations of the compounds for 24 h, and Western blot analysis was performed using specific antibodies: FL-PARP, full-length PARP; Cl-PARP, cleaved PARP; Pro-Cas3, pro-caspase-3; Cl-Cas3, cleaved caspase-3.

had an IC_{50} of >10 μM in the HCT-116 p53$^{-/-}$ cell line, thus displaying >100-fold selectivity for the HCT-116 cell line with wild-type p53 over its isogenic p53 deleted cell line.

Encouraged by its promising in vitro activity and excellent oral PK profile, we evaluated **9** for its antitumor activity in the SJSA-1 osteosarcoma and RS4;11 acute leukemia xenograft models in SCID mice.

In the efficacy experiment using the SJSA-1 xenograft model, SJSA-1 tumors were grown to approximately 100 mm^3 and **9** was administered via oral gavage to mice daily for 2 weeks at 10, 30, and 100 mg/kg (Figure 5). While **9** had no significant activity at 10 mg/kg, it effectively inhibited tumor growth at 30

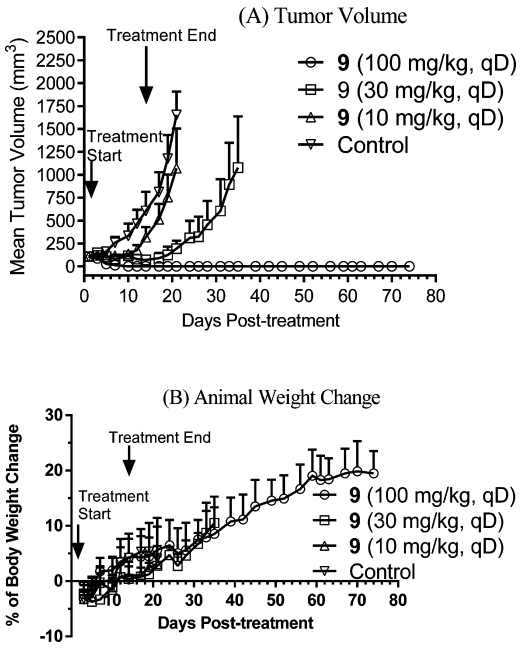

Figure 5. Antitumor activity of **9** in the SJSA-1 osteosarcoma tumor xenograft model in mice: (A) tumor volume; (B) animal weight change.

dx.doi.org/10.1021/jm4005708 | J. Med. Chem. 2013, 56, 5553–5561

mg/kg. Impressively, **9** at 100 mg/kg achieved rapid and complete tumor regression. After 5 days of daily dosing, the average tumor volume was decreased by >70%, and after 10 days of dosing, all the mice (8 out of 8 mice) treated with **9** had undetectable tumor. The complete tumor regression was durable; all the mice remained tumor free for 60 days after the last dose. There was no significant difference in animal weight between the vehicle control group of mice and the three groups of mice treated with **9**. Furthermore, there was minimal weight loss and no sign of toxicity observed in mice treated with **9** at all doses during the entire experiment. Collectively, these data showed that **9** was well tolerated in mice at all the doses tested.

To gain an insight into the in vivo mechanism of action of **9**, we tested its ability and kinetics in activation of p53 and induction of apoptosis in the SJSA-1 xenograft tissue (Figure 6). Mice bearing SJSA-1 xenograft tumors were given a single oral dose of **9** at 100 mg/kg. Mice were then sacrificed at different time points, and tumors were harvested for Western blot analysis. Our Western blot data showed that **9** induced robust up-regulation of p53, as well as p21 and MDM2 proteins at 3 and 6 h time points, indicative of strong p53 activation in tumor tissue. The levels of p53, p21, and MDM2 proteins were significantly diminished at the 24 h time point, suggesting that p53 activation was transient in tumor tissue. Interestingly, cleavage of PARP and caspase-3 was minimal at the 1, 3, and 6 h time points but became very clear at the 24 h time point, indicating that while p53 was activated by **9** in tumor tissue quickly, apoptosis induction occurred at later time points.

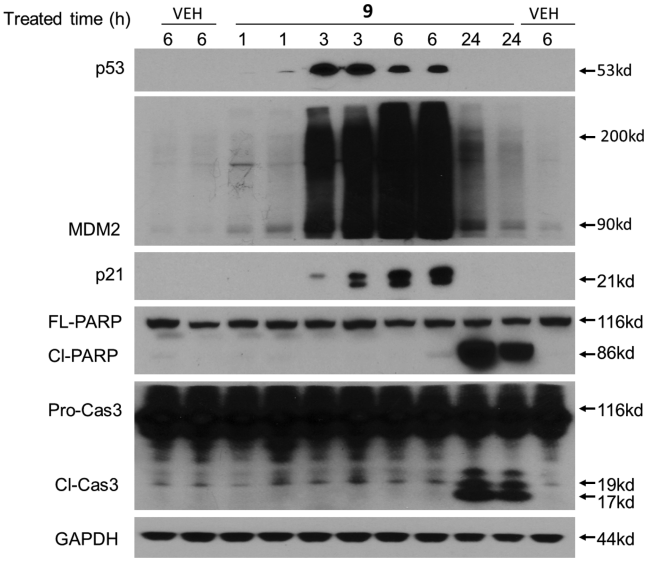

Figure 6. Activation of p53 and cleavage of caspase-3 and PARP in SJSA-1 tumor tissue by **9**. Mice bearing SJSA-1 tumors were dosed with a single oral dose of **9** at 100 mg/kg, and tumor tissue was harvested at different time points for Western blot analysis using specific antibodies: FL-PARP, full-length PARP; Cl-PARP, cleaved PARP; Pro-Cas3, pro-caspase-3; Cl-Cas3, cleaved caspase-3.

In the efficacy experiment using the RS4;11 acute leukemia xenograft model, when tumors grew to an average volume of 150 mm^3, compound **9** was administered at 100 and 200 mg/kg via oral gavage daily for 3 weeks (Figure 7). At both 100 and 200 mg/kg, **9** achieved rapid and complete tumor regression. After 4 days of dosing, tumor volume was decreased by 61% and 80% with the treatment at 100 and 200 mg/kg,

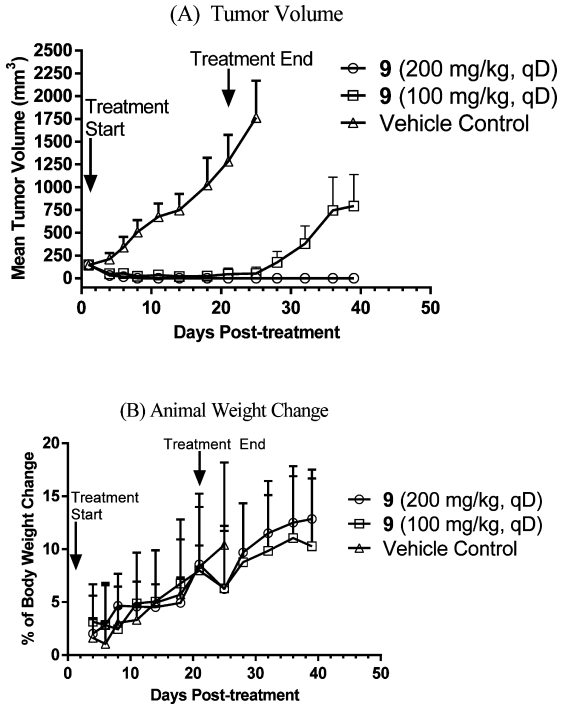

Figure 7. Antitumor activity of **9** in the RS4;11 acute lymphoblastic leukemia xenograft model: (A) tumor volume; (B) animal weight change.

respectively. Complete tumor regression was observed in all the animals after 7 days of dosing with **9** at 200 mg/kg. The complete tumor regression was also durable; 26 days after the last dose, all mice treated with **9** at 200 mg/kg still remained tumor free. There was no significant weight loss or other signs of toxicity for all the mice treated with **9** during the entire experiment.

CHEMISTRY

The synthesis of **3**–**10** is shown in Scheme 1. The synthesis of **9** has been reported in a previous communication.[21]

Compound **12** was synthesized using previously reported methods.[11−13,21] Most amines required for the synthesis of intermediate **13** were commercially available with the exception of **8**, **9**, and **10**. The intermediate **14** was synthesized according to previously reported procedures.[11−13,21] Compound **14** was isomerized in MeCN−H_2O or MeOH for 3−4 days, affording final compounds in 50−60% yield as determined by analytical HPLC or UPLC.

The *trans*-*N*-(3-aminocyclobutanyl)methylsulfonamide **17** used for the synthesis of **10** was synthesized from commercially available material **15** (Scheme 2). Compound **15** was converted into mesylate **16** in 84% yield and the *N*-Boc group was cleaved in TFA−CH_2Cl_2 solution, affording **17**. The amine **17** was neutralized using 2 N NaOH aqueous solution prior to use.

CONCLUSION

In the present study, we designed and synthesized a set of new and potent MDM2 inhibitors with the goal to improve the oral pharmacokinetics profile over **2** by constraining the conformation of the 1,2-diol moiety and blocking the metabolic oxidative site. Among these new compounds, **9** is a highly potent MDM2 inhibitor and has an excellent oral pharmacokinetics profile. Significantly, **9** is capable of achieving complete

dx.doi.org/10.1021/jm4005708 | J. Med. Chem. 2013, 56, 5553−5561

Scheme 1. General Synthetic Route for Final Compounds[a]

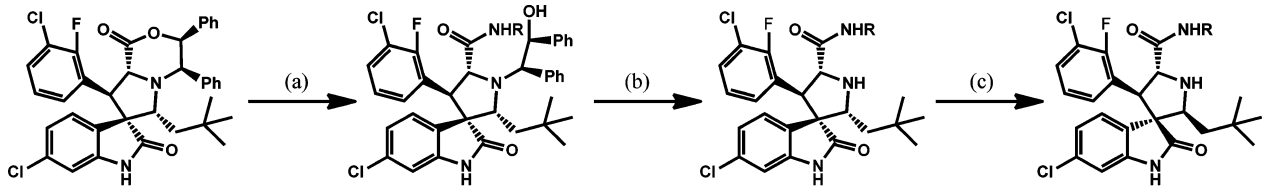

[a]Reagents and conditions: (a) free amine, 1.0−2.0 equiv, THF, rt, 12 h; (b) 2.1 equiv of ammonium cerium(IV) nitrate (CAN), MeCN/H_2O = 1:1, rt, 1 h; (c) $NaHCO_3$, MeOH−H_2O = 1:1, 3−4 days.

Scheme 2. Synthesis of *trans*-*N*-(3-Aminocyclobutanyl)methylsulfonamide 17[a]

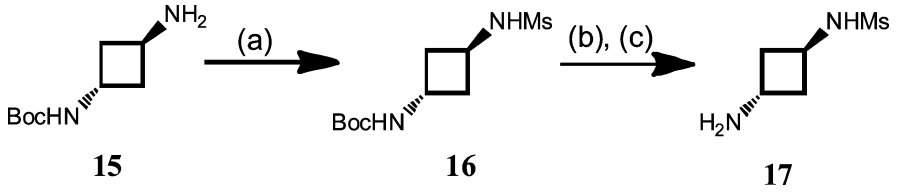

[a]Reagents and conditions: (a) MsCl, Et_3N, THF, 0 °C to rt, 84%; (b). TFA, CH_2Cl_2, rt, 1 h; (c) NaOH, MeOH−H_2O.

and durable tumor regression in both SJSA-1 osteosarcoma and RS4;11 acute lymphoblastic leukemia tumor xenograft models. Our in vitro and in vivo data show that **9** is a promising MDM2 inhibitor and warrants extensive evaluation as a potential clinical development candidate for the treatment of human cancer.

EXPERIMENTAL SECTION

General Chemistry. All reactions were conducted in a round-bottom flask equipped with a Teflon-coated magnetic stirring bar. Experiments involving moisture and/or air sensitive components were performed under a nitrogen atmosphere. Commercial reagents and anhydrous solvents were used without further purification. The crude reaction product was purified by flash column chromatography packed with silica gel. Further purification was performed on a semipreparative HPLC instrument (Waters Delta 600) with a SunFire C18 reverse phase column (19 mm × 150 mm). The mobile phase was a gradient flow of solvent A (water, 0.1% of TFA) and solvent B (CH_3CN, 0.1% of TFA or MeOH, 0.1% of TFA) at a flow rate of 10 mL/min. Proton nuclear magnetic resonance (^{1}H NMR) spectroscopy and carbon nuclear magnetic resonance (^{13}C NMR) spectroscopy were performed in Bruker Advance 300 NMR spectrometers. Low resolution ESI mass spectrum analysis was performed on a Thermo-Scientific LCQ Fleet mass spectrometer. The analytical HPLC model was a Waters 2795 Separation (UV detection at 230 and 254 nm wavelengths) using the reverse phase column (SunFire, C18-5 μm, 4.6 mm × 150 mm). The analytical UPLC model was Waters Acquity H class (UV detection at 230 and 254 nm wavelengths). The reverse phase column used was the Acquity UPLC BEH (C18-1.7 μm, 2.1 mm × 50 mm). All final compounds were purified to ≥95% purity as determined by analytical UPLC or HPLC analysis. The optical rotation was measured on an Autopol III automatic polarimeter (Rudolph Research Analytical). The specific optical rotation was calculated by application of the following formula: $[\alpha]_D^T = \alpha/(lc)$, where α is the observed angular rotation, l is the length of the cell in decimeters (l = 1 dm), and c is the concentration in grams per milliliter (g/mL).

Synthesis of **3** from the corresponding intermediate **14** (Scheme 1, R = *trans*-3-hydroxycyclobutyl) was through isomerization: **14** (60 mg) obtained from CAN oxidation was placed in a round-bottom flask equipped with magnetic stirring bar. MeOH (5 mL) was added to dissolve **14**, followed by water (4 mL) and saturated $NaHCO_3$ solution (0.5 mL) to set the pH at 8−9. This solution was stirred at room temperature for 3−4 days, and **3** constituted 52% of all four isomers as determined by UPLC analysis. Final purification of **3** was performed using semipreparative or preparative reverse phase HPLC. The isomerization and purification of **4**−**8** and **10** followed the same isomerization procedure.

(2′*S*,3*R*,4′*S*,5′*R*)-6-Chloro-4′-(3-chloro-2-fluorophenyl)-*N*-(*trans*-3-hydroxycyclobutyl)-2′-neopentyl-2-oxospiro-[indoline-3,3′-pyrrolidine]-5′-carboxamide (3). ^{1}H NMR (300 MHz, MeOD-d_4): 8.77 (d, J = 5.78 Hz, 1H, NH), 7.64−7.52 (m, 2H), 7.41 (t, J = 6.85 HZ, 1H), 7.23−7.13 (m, 1H), 7.14 (dd, J = 8.11, 1.82 Hz, 1H), 6.79 (d, J = 1.77 Hz, 1H), 5.21 (d, J = 11.34 Hz, 1H), 4.58 (d, J = 11.34 Hz, 1H), 4.50 (dd, J = 8.22, 1.94 Hz, 1H), 4.34−4.22 (m, 1H), 4.20−4.06 (m, 1H), 2.30−2.06 (m, 3H), 1.94−1.80 (m, 2H), 1.15 (dd, J = 15.13, 1.70 Hz, 1H), 0.87 (s, 9H). ^{13}C NMR (75 MHz, MeOD-d_4): 177.87, 167.38, 157.87 (d, J_{C-F} = 245.04 Hz), 145.18, 137.29, 132.68, 128.70, 126.79, 126.63 (d, J_{C-F} = 4.91 Hz), 124.22, 123.47, 122.63 (d, J_{C-F} = 18.68 Hz), 121.64 (d, J_{C-F} =13.39 Hz), 112.17, 65.20, 64.67, 64.27, 62.88, 43.46, 42.97, 40.40, 39.83, 31.01, 29.59. ESI-MS calculated for $C_{27}H_{31}{}^{35}Cl_2FN_3O_3$ $[M + H]^+$: 534.17. Found: 534.14.

To a round-bottom flask, **12** (2.9 g, 4.50 mmol), *cis*-3-amino-cyclobutanol (0.40 g, 4.56 mmol), and THF (30 mL) were added, and the solution was stirred at room temperature for 12 h. THF was removed, and the crude material was purified on flash column chromatography. The desired ring-opening adduct was isolated in 2.13 g (2.93 mmol). The ring-opening adduct and MeCN (20 mL) were placed in a round-bottom flask. CAN (3.37 g, 6.15 mmol) and water (20 mL) were subsequently added, and the mixture was stirred at room temperature for 1 h before quenching with $NaHCO_3$ saturated solution. The aqueous layer was extracted with ethyl acetate (50 mL × 3), and the combined organic layers were washed with water and brine and dried over anhydrous Na_2SO_4. The solvent was removed, and the crude material was purified on flash column chromatography. The corresponding intermediate **14** was isolated in 624 mg (1.17 mmol, 26% yield over two steps). **4** constituted 56% of all four isomers upon isomerization of **14** (Scheme 1, R = *cis*-3-hydroxycyclobutyl) for 3 days.

(2′*S*,3*R*,4′*S*,5′*R*)-6-Chloro-4′-(3-chloro-2-fluorophenyl)-*N*-(*cis*-3-hydroxycyclobutyl)-2′-neopentyl-2-oxospiro[indoline-3,3′-pyrrolidine]-5′-carboxamide (4). ^{1}H NMR (300 MHz, MeOD-d_4): 8.77 (d, J = 6.95 Hz, 1H), 7.62−7.51 (m, 2H), 7.37 (d, J = 7.00 Hz, 1H), 7.20−7.12 (m, 1H), 7.12 (dd, J = 8.02, 1.74 Hz, 1H), 6.78 (d, J = 1.68 Hz, 1H), 5.23 (d, J = 11.33 Hz, 1H), 4.60 (d, J = 11.33 Hz, 1H), 4.50 (dd, J = 8.24, 1.49 Hz, 1H), 3.98−3.84 (m, 1H), 3.84−3.70 (m, 1H), 2.64 (ddd, J = 12.94, 12.71, 6.64 Hz, 1H), 2.50 (ddd, J = 12.46, 12.50, 6.55 Hz, 1H), 1.90 (dd, J = 15.46, 8.33 Hz,

dx.doi.org/10.1021/jm4005708 | J. Med. Chem. 2013, 56, 5553−5561

1H), 1.80 (dd, J = 19.42, 8.81 Hz, 1H), 1.53 (dd, J = 19.42, 8.81 Hz, 1H), 1.13 (dd, J = 15.46, 1.46 Hz, 1H), 0.86 (s, 9H). ^{13}C NMR (75 MHz, MeOD-d_4): 177.78, 166.96, 157.86 (d, J_{C-F} = 249.82 Hz), 145.19, 137.24, 132.58, 128.67, 126.79, 126.58 (d, J_{C-F} = 4.98 Hz), 124.15, 123.47, 122.55 (d, J_{C-F} = 18.94 Hz), 121.58 (d, J_{C-F} = 12.97 Hz), 112.15, 64.55, 64.26, 62.72, 61.22, 43.37, 41.44, 41.36, 38.05, 30.97, 29.56. ESI-MS calculated for $C_{27}H_{31}{}^{35}Cl_2FN_3O_3$ [M + H]$^+$: 534.17. Found: 534.28. $[\alpha]_D^{25}$ −16.7° (MeOH, c 0.0160 g/mL).

To a round-bottom flask, **12** (3.2 g, 4.95 mmol), (1*R*,3*S*)-3-aminocyclopentanol (0.5 g, 4.95 mmol), and THF (25 mL) were added, and the solution was stirred at room temperature for 12 h. THF was removed, and the crude material was purified on flash column chromatography. The desired ring-opening adduct was isolated in 2.68 g (3.46 mmol). The ring-opening adduct and MeCN (20 mL) were placed in a round-bottom flask. CAN (3.98 g, 7.27 mmol) and water (20 mL) were subsequently added, and the mixture was stirred at room temperature for 1 h before quenching with $NaHCO_3$ saturated solution. The aqueous layer was extracted with ethyl acetate (50 mL × 3), and the combined organic layers were washed with water and brine and dried over anhydrous Na_2SO_4. The solvent was removed, and the crude material was purified on flash column chromatography. The corresponding intermediate **14** was isolated in 811 mg (1.48 mmol, 30% yield over two steps). **5** constituted 64% of all four isomers upon isomerization of **14** (Scheme 1, R = (1*S*,3*R*)-3-hydroxycyclopentyl) for 3 days.

(2′*S*,3*R*,4′*S*,5′*R*)-6-Chloro-4′-(3-chloro-2-fluorophenyl)-*N*-((1*S*,3*R*)-3-hydroxycyclopentyl)-2′-neopentyl-2-oxospiro-[indoline-3,3′-pyrrolidine]-5′-carboxamide (5). ^{1}H NMR (300 MHz, MeOD-d_4): 8.24 (d, J = 7.50 Hz, 1H, NH), 7.63−7.52 (m, 2H), 7.37 (t, J = 6.96 Hz, 1H), 7.19−7.11 (m, 1H), 7.12 (dd, J = 8.10, 1.78 Hz, 1H), 6.78 (d, J = 1.70 Hz, 1H), 5.28 (d, J = 11.52 Hz, 1H), 4.60 (d, J = 11.52 Hz, 1H), 4.51 (dd, J = 8.35, 1.65 Hz, 1H), 4.26−4.08 (m, 2H), 2.20−2.06 (m, 1H), 1.91 (dd, J = 15.44, 8.35 Hz, 1H), 1.84−1.60 (m, 2H), 1.56−1.40 (m, 2H), 1.38−1.24 (m, 1H), 1.14 (dd, J = 15.37, 1.48 Hz, 1H), 0.87 (s, 9H). ^{13}C NMR (75 MHz, MeOD-d_4): 177.78, 166.74, 157.91 (d, J_{C-F} = 249.49 Hz), 145.18, 137.23, 132.26, 128.67, 126.74, 126.67 (d, J_{C-F} = 4.93 Hz), 124.15, 123.50, 122.62 (d, J_{C-F} = 19.14 Hz), 121.61 (d, J_{C-F} = 12.95 Hz), 112.16, 73.04, 64.43, 64.30, 62.82, 51.66, 43.41, 42.00, 34.65, 31.79, 30.99, 29.56. ESI-MS calculated for $C_{28}H_{33}{}^{35}Cl_2FN_3O_3$ [M + H]$^+$: 548.19. Found: 548.20. $[\alpha]_D^{25}$ −18.7° (MeOH, c 0.0174 g/mL).

The same procedure for the synthesis of **5** was followed using (1*S*,3*S*)-3-aminocyclopentanol as the reactant. The CAN oxidation furnished the corresponding intermediate **14** in 32% over two steps. **6** constituted 70% of all four isomers upon isomerization of **14** (Scheme 1, R = (1*S*,3*S*)-3-hydroxycyclopentyl) for 3 days.

(2′*S*,3*R*,4′*S*,5′*R*)-6-Chloro-4′-(3-chloro-2-fluorophenyl)-*N*-((1*S*,3*S*)-3-hydroxycyclopentyl)-2′-neopentyl-2-oxospiro-[indoline-3,3′-pyrrolidine]-5′-carboxamide (6). ^{1}H NMR (300 MHz, MeOD-d_4): 8.47 (d, J = 7.23 Hz, 1H, NH), 7.68−7.54 (m, 2H), 7.41 (t, J = 6.94 Hz, 1H), 7.24−7.14 (m, 1H), 7.16 (dd, J = 8.13, 1.82 Hz, 1H), 6.81 (d, J = 1.74 Hz, 1H), 5.23 (d, J = 11.38 Hz, 1H), 4.61 (d, J = 11.38 Hz, 1H), 4.54 (dd, J = 8.22, 1.64 Hz, 1H), 4.42−4.28 (m, 1H), 4.28−4.19 (m, 1H), 2.04−1.86 (m, 3H), 1.80−1.60 (m, 2H), 1.56−1.42 (m, 1H), 1.17 (dd, J = 15.34, 1.39 Hz, 1H), 1.14−1.00 (m, 1H), 0.89 (s, 9H). ^{13}C NMR (75 MHz, MeOD-d_4): 177.81, 167.10, 157.86 (d, J_{C-F} = 248.99 Hz), 145.17, 137.22, 132.57, 128.75, 126.79, 126.61 (d, J_{C-F} = 4.71 Hz), 124.18, 123.54, 122.54 (d, J_{C-F} = 18.86 Hz), 121.63 (d, J_{C-F} = 12.93 Hz), 112.16, 72.88, 64.59, 64.13, 62.89, 51.52, 51.41, 43.44, 42.29, 34.30, 31.61, 30.99, 29.57. ESI-MS calculated for $C_{28}H_{33}{}^{35}Cl_2FN_3O_3$ [M + H]$^+$: 548.19. Found: 548.32. $[\alpha]_D^{25}$ −22.9° (MeOH, c 0.0112 g/mL).

To a round-bottom flask, **12** (3.0 g, 4.67 mmol), 1-amino-2-methylpropan-2-ol (0.41 g, 4.60 mmol), and THF (25 mL) were added, and the solution was stirred at room temperature for 12 h. THF was removed, and the crude material was purified on flash column chromatography. The desired ring-opening adduct was isolated in 2.19 g (2.99 mmol). The ring-opening adduct and MeCN (10 mL) were placed in a round-bottom flask. CAN (3.44 g, 6.28 mmol) and water (10 mL) were subsequently added, and the mixture was stirred at room temperature for 1 h before quenching with $NaHCO_3$ saturated solution. The aqueous layer was extracted with ethyl acetate (50 mL × 3), and the combined organic layers were washed with water and brine and dried over anhydrous Na_2SO_4. The solvent was removed, and the crude material was purified on flash column chromatography. The corresponding intermediate **14** was isolated in 690 mg (1.29 mmol, 28% over two steps). **7** constituted 62% of all four isomers upon isomerization of **14** (Scheme 1, R = 2-hydroxy-2-methylpropyl) for 3 days.

(2′*S*,3*R*,4′*S*,5′*R*)-6-Chloro-4′-(3-chloro-2-fluorophenyl)-*N*-(2-hydroxy-2-methylpropyl)-2′-neopentyl-2-oxospiro[indoline-3,3′-pyrrolidine]-5′-carboxamide (7). ^{1}H NMR (300 MHz, MeOD-d_4): 7.65−7.56 (m, 2H), 7.35 (t, J = 7.04 Hz, 1H), 7.20−7.14 (m, 1H), 7.12 (dd, J = 8.02, 1.66 Hz, 1H), 6.78 (d, J = 1.64 Hz, 1H), 5.42 (d, J = 11.51 Hz, 1H), 4.64 (d, J = 11.51 Hz, 1H), 4.54 (dd, J = 8.22, 1.27 Hz, 1H), 3.40−3.30 (m, 1H), 2.98 (d, J = 13.44 Hz, 1H), 1.93 (dd, J = 15.42, 8.38 Hz, 1H), 1.14 (dd, J = 15.45, 1.18 Hz, 1H), 0.97 (s, 3H), 0.87 (s, 9H), 0.83 (s, 3H). ^{13}C NMR (75 MHz, MeOD-d_4): 177.70, 168.15, 157.90 (d, J_{C-F} = 249.83 Hz), 145.20, 137.21, 132.57, 128.83, 126.83, 126.68 (d, J_{C-F} = 4.69 Hz), 124.13, 123.51, 122.66 (d, J_{C-F} = 18.96 Hz), 121.63 (d, J_{C-F} = 13.25 Hz), 112.16, 75.58, 71.16, 64.48, 64.43, 62.85, 51.51, 43.45, 31.01, 29.58, 27.41, 26.65. ESI-MS calculated for $C_{27}H_{33}{}^{35}Cl_2FN_3O_3$ [M + H]$^+$: 536.19. Found: 536.44. $[\alpha]_D^{25}$ −24.0° (MeOH, c 0.0186 g/mL).

To a round-bottom flask, **12** (643 mg, 1.0 mmol), *trans*-3-(*tert*-butyldimethylsilyloxy)-3-methylcyclobutanamine[21] (0.10 g, 0.46 mmol), and THF (10 mL) were added, and the solution was stirred at room temperature for 12 h. THF was removed, and the crude material was purified on flash column chromatography. The desired ring-opening adduct was isolated in 0.36 g (0.41 mmol). The ring-opening adduct and MeCN (5 mL) were placed in a round-bottom flask. CAN (450 mg, 0.82 mmol) and water (5 mL) were subsequently added, and the mixture was stirred at room temperature for 1 h before quenching with $NaHCO_3$ saturated solution. The aqueous layer was extracted with ethyl acetate (50 mL × 3), and the combined organic layers were washed with water and brine and dried over anhydrous Na_2SO_4. The solvent was removed, and the crude material was purified on flash column chromatography. The corresponding intermediate **14** was isolated in 62 mg (0.11 mmol, 24% yield over two steps), and (2′*S*,3*R*,4′*S*,5′*R*)-*N*-((1*r*,3*R*)-3-((*tert*-butyldimethylsilyl)oxy)-3-methylcyclobutyl)-6-chloro-4′-(3-chloro-2-fluorophenyl)-1′-((1*R*,2*S*)-2-hydroxy-1,2-diphenylethyl)-2′-neopentyl-2-oxospiro[indoline-3,3′-pyrrolidine]-5′-carboxamide was also isolated (chiral-auxiliary-cleaved product with the hydroxy group protected by TBS, 53 mg, 0.08 mmol, 17% yield over two steps). **8** constituted 64% of all four isomers upon isomerization of **14** (Scheme 1, R = *trans*-3-hydroxy-3-methylcyclobutyl) for 3 days.

(2′*S*,3*R*,4′*S*,5′*R*)-6-Chloro-4′-(3-chloro-2-fluorophenyl)-*N*-(*trans*-3-hydroxy-3-methylcyclobutyl)-2′-neopentyl-2-oxospiro[indoline-3,3′-pyrrolidine]-5′-carboxamide (8). ^{1}H NMR (300 MHz, MeOD-d_4): 8.68 (d, J = 5.95 Hz, 1H, NH), 7.64−7.52 (m, 2H), 7.41 (t, J = 7.56 Hz, 1H), 7.24−7.14 (m, 1H), 7.14 (dd, J = 8.06, 1.64 Hz, 1H), 6.79 (d, J = 1.76 Hz, 1H), 5.19 (d, J = 11.28 Hz, 1H), 4.58 (d, J = 11.28 Hz, 1H), 4.50 (dd, J = 8.06, 1.65 Hz, 1H), 4.37−4.20 (m, 1H), 2.44−2.22 (m, 2H), 1.96−1.82 (m, 2H), 1.62 (dd, J = 11.69, 5.79 Hz, 1H), 1.15 (dd, J = 15.43, 1.66 Hz, 1H), 1.09 (s, 3H), 0.87 (s, 9H). ^{13}C NMR (75 MHz, MeOD-d_4): 177.84, 167.28, 157.90 (d, J_{C-F} = 249.25 Hz), 145.17, 137.28, 132.66, 128.70, 126.79, 126.68 (d, J_{C-F} = 4.96 Hz), 124.20, 123.41, 122.65 (d, J_{C-F} = 18.90 Hz), 121.63 (d, J_{C-F} = 12.76 Hz), 112.16, 70.79, 64.65, 64.25, 62.84, 44.80, 43.73, 43.39, 40.89, 30.97, 29.56, 29.43. ESI-MS calculated for $C_{28}H_{33}{}^{35}Cl_2FN_3O_3$ [M + H]$^+$: 548.19. Found: 548.56.

To a round-bottom flask, **12** (1.286 g, 2.0 mmol), **17** (1.8 mmol based on **16**), and THF (15 mL) were added, and the solution was stirred at room temperature for 12 h. THF was removed, and the crude material was purified on flash column chromatography. The desired ring-opening adduct was isolated in 0.776 g (0.96 mmol). The ring-opening adduct and MeCN (10 mL) were placed in a round-bottom flask. CAN (1.053 g, 1.84 mmol) and water (10 mL) were subsequently added, and the mixture was stirred at room temperature

for 1 h before quenching with $NaHCO_3$ saturated solution. The aqueous layer was extracted with ethyl acetate (50 mL × 3), and the combined organic layers were washed with water and brine and dried over anhydrous Na_2SO_4. The solvent was removed, and the crude material was purified on flash column chromatography. The corresponding intermediate **14** was isolated in 626 mg (1.023 mmol, 56% yield over two steps). **10** constituted 62% of all four isomers upon isomerization of **14** (Scheme 1, R = *trans*-3-(methylsulfonamido)-cyclobutyl) for 3 days.

(2′*S*,3*R*,4′*S*,5′*R*)-6-Chloro-4′-(3-chloro-2-fluorophenyl)-*N*-(*trans*-3-(methylsulfonamido)cyclobutyl)-2′-neopentyl-2-oxospiro[indoline-3,3′-pyrrolidine]-5′-carboxamide (10). ^{1}H NMR (300 MHz, MeOD-d_4): 8.96 (d, J = 6.37 Hz, 1H, NH), 7.64−7.54 (m, 2H), 7.36 (t, J = 6.96 Hz, 1H), 7.20−7.16 (m, 1H), 7.11 (dd, J = 8.13, 1.79 Hz, 1H), 6.78 (d, J = 1.75 Hz, 1H), 5.32 (d, J = 11.51 Hz, 1H), 4.63 (d, J = 11.51 Hz, 1H), 4.52 (d, J = 8.47, 1.49 Hz, 1H), 4.28−4.14 (m, 1H), 3.83 (quintet, J = 3.83 Hz, 1H), 2.84 (s, 3H), 2.40−2.30 (m, 2H), 2.30−2.20 (m, 1H), 2.06−1.96 (m, 1H), 1.93 (dd, J = 15.47, 8.42 Hz, 1H), 1.13 (dd, J = 15.47, 1.23 Hz, 1H), 0.86 (s, 9H). ^{13}C NMR (75 MHz, MeOD-d_4): 177.73, 167.29, 157.80 (d, J_{C-F} = 249.64 Hz), 145.13, 137.16, 132.63, 128.69, 126.75, 126.61 (d, J_{C-F} = 4.84 Hz), 124.13, 123.52, 122.51 (d, J_{C-F} = 18.77 Hz), 121.55 (d, J_{C-F} = 13.01 Hz), 112.15, 64.51, 64.11, 62.70, 46.60, 43.43, 40.93, 38.47, 38.11, 30.97, 29.54. ESI-MS calculated for $C_{28}H_{34}{}^{35}Cl_2FN_4O_4S$ $[M + H]^+$: 611.17. Found: 611.42. $[\alpha]_D^{25}$ −13.8° (MeOH, *c* 0.0208 g/mL).

***N*-(*trans*-3-Aminocyclobutyl)methanesulfonamide (17).** To a round-bottom flask, **15** (400 mg, 2.15 mmol, 1.0 equiv), Et_3N (1 mL, 7.5 mmol, 3.5 equiv), and THF (25 mL) were added. The reaction mixture was cooled in an ice−water bath, and methanesulfonyl chloride (MsCl, 492 mg, 4.3 mmol, 2.0 equiv) was added dropwise via a syringe. The mixture was stirred at room temperature for 12 h before quenching with water. The aqueous layer was extracted with ethyl acetate (70 mL × 2), and the combined organic layers were washed with brine (50 mL) and dried over anhydrous Na_2SO_4. The solvents were removed, and the crude product was purified on flash column chromatography. **16** was obtained as a white solid (0.475 g, 84%). **16**: ^{1}H NMR (MeOD-d_4, 300 MHz) 4.10−3.92 (m, 2H), 2.87 (s, 3H), 2.30 (t, J = 6.71 Hz, 4H), 1.43 (s, 9H) ^{13}C (MeOD-d_4, 75 M Hz): 158.07, 80.52, 46.61, 43.58, 40.90, 38.90, 28.91. ESI-MS: calculated for $C_{10}H_{20}N_2NaO_4S$ $[M + Na]^+$ = 287.10; obtained, 287.16.

To a round-bottom flask, **16** (0.475 g, 1.8 mmol), Et_3SiH (0.1 mL), and CH_2Cl_2 (15 mL) were added. TFA (4 mL) was added via a syringe, and the mixture was stirred at room temperature for 1 h. The reaction mixture was concentrated to remove solvent and TFA. MeOH (15 mL) was added, and the pH was adjusted to be 10−11 by NaOH (2 N aqueous solution). MeOH and water were then removed affording crude free amine **17**, which was directly used for the next step without further purification.

FP-Based Protein Binding Assay. The binding affinity of MDM2 inhibitors was determined by an optimized, sensitive, and quantitative fluorescence-polarization-based (FP-based) binding assay using a recombinant human His-tagged MDM2 protein (residues 1−118) and a FAM tagged p53-based peptide as the fluorescent probe. The design of the fluorescent probe was based upon a previously reported high affinity p53-based peptidomimetic compound (5-FAM-βAla-βAla-Phe-Met-Aib-pTyr-(6-Cl-LTrp)-Glu-Ac3c-Leu-Asn-NH_2).[22] This tagged peptide was named PMDM6-F. The K_d value of PMDM6-F to the MDM2 protein was determined to be 1.4 ± 0.3 nM by monitoring the total fluorescence polarization of mixtures composed with the fluorescent probe at a fixed concentration and the MDM2 protein with increasing concentrations up to full saturation. Fluorescence polarization values were measured using the Infinite M-1000 plate reader (Tecan U.S., Research Triangle Park, NC) in Microfluor 2 96-well, black, round-bottom plates (Thermo Scientific). In the saturation experiments, 1 nM PMDM6-F and increasing concentrations of proteins were added to each well to a final volume of 125 μL in the assay buffer (100 mM potassium phosphate, pH 7.5, 100 μg/mL bovine γ-globulin, 0.02% sodium azide [Invitrogen], with 0.01% Triton X-100 and 4% DMSO). Plates were mixed and incubated at room temperature for 15−30 min with gentle shaking to ensure equilibrium. The polarization values in millipolarization units (mP) were measured at an excitation wavelength of 485 nm and an emission wavelength of 530 nm. Equilibrium dissociation constants (K_d) were then calculated by fitting the sigmoidal dose-dependent FP increases as a function of protein concentrations using Graphpad Prism 5.0 software (Graphpad Software, San Diego, CA). K_i values of tested compounds were determined in a dose-dependent competitive binding experiment. Mixtures of 5 μL of the tested compound in different concentrations in DMSO and 120 μL of preincubated protein/fluorescent probe complex with fixed concentrations in the assay buffer (100 mM potassium phosphate, pH 7.5, 100 μg/mL bovine γ-globulin, 0.02% sodium azide, with 0.01% Triton X-100) were added into assay plates and incubated at room temperature with gentle shaking. The incubation time was precisely controlled at 15 min to minimize the influence of the initial isomerization to the binding affinities. Final concentrations of the protein and fluorescent probe in the competitive assays were 10 and 1 nM, respectively, and final DMSO concentration is 4%. Negative controls containing protein/fluorescent probe complex only (equivalent to 0% inhibition), and positive controls containing free fluorescent probe only (equivalent to 100% inhibition), were included in each assay plate. FP values were measured as described above. IC_{50} values were determined by nonlinear regression fitting of the sigmoidal dose-dependent FP decreases as a function of total compound concentrations using Graphpad Prism 5.0 software (Graphpad Software, San Diego, CA). K_i values of tested compounds to the MDM2 protein were calculated using the measured IC_{50} values, the K_d value of the fluorescent probe to the protein, and the concentrations of the protein and fluorescent probe in the competitive assays.[23]

Cell Growth Inhibition Assay. The SJSA-1 osteosarcoma cell line and RS4;11 leukemia cell line were purchased from the American Type Culture Collection (Manassas, VA). HCT-116 $p53^{+/+}$ colon cell line (HCT-116 $p53^{+/+}$) and its isogenic p53 knockout (HCT-116 $p53^{-/-}$) cell line are kind gifts from Dr. Bert Vogelstein, Johns Hopkins University at Baltimore, MD. All cell lines were grown in PRMI 1640 medium (Gibco, Life Technologies, Grand Island, NY) supplemented with 10% FBS (Invitrogen, Carlsbad, CA) in a humidified tissue culture incubator at 37 °C, 5% CO_2. For cell growth inhibition assay, cells were seeded in 96-well, flat-bottom cell culture plates at a density of (3−4) × 10^3 cells/well and allowed to grow overnight, then incubated with a compound at different concentrations. The effect of cell growth inhibition of a compound was determined with a lactate dehydrogenase based WST-8 assay (WST-8; Dojindo Molecular Technologies Inc., Gaithersburg, MD). For the RS4;11 cell line, WST-8 solution was directly added to culture medium in each well to a final concentration of 10% upon the end of treatment. For SJSA-1, HCT-116 $p53^{+/+}$, and HCT-116 $p53^{-/-}$, culture medium in each well was discharged and fresh RPMI 1640 medium with no phenol red (Gibco, life Technologies, Grand Island, NY) containing 10% WST-8 solution was added to each well in the presence of 5% FBS upon the end of treatment. Then the plates were incubated at 37 °C for 2−3 h. The absorbance of the samples was measured at 450 nm using a TECAN ULTRA reader. The effect of each treatment was calculated by the equation [(absorbance value of treatment) − (absorbance value of medium with FBS + WST solution only)]/[(absorbance value of untreated control) − (absorbance value of medium with FBS + WST solution only)]. The IC_{50} value of a compound is the concentration that inhibits cell growth by 50% over the control.

Pharmacodynamics (PD) Study. For PD studies, the SJSA-1 xenograft tumor model was used. To develop xenograft tumors, 5 × 10^6 SJSA-1 cancer cells with 50% Matrigel were injected sc on the dorsal side of SCID mice from Charles River, one tumor per mouse. When xenograft tumors reached a mean of ∼100 mm^3 (70−130 mm^3), two mice were treated with vehicle control (10% PEG400/3% Cremophor/87% PBS) and eight mice were treated with a single dose of **9** at 100 mg/kg via oral gavage. Mice treated with vehicle control were sacrificed at 6 h, and tumor tissue was harvested for Western blot

analysis. Two mice treated with **9** were sacrificed at 1, 3, 6, and 24 h (two mice at each time point), and tumor tissue was harvested.

Western Blotting. For Western blot analysis, tumor cells or tumor tissues were lysed in ice-cold RIPA buffer: 20 mM Tris-HCl (pH 7.5), 150 mM NaCl, 1 mM EDTA, 1 mM EGTA, 1% sodium deoxycholate, 2.5 mM sodium pyrophosphate, 1 mM β-glycerophosphate, 1 mM sodium orthovanadate, and 1 μg/mL leupeptin. The expressions of indicated proteins in the whole cell lysates were detected by Western blot analysis using the following antibodies: anti-p53 (OP43, Calbiochem), anti-MDM2 (sc-965, Santa Cruz), anti-p21 (556431, BD Biosciences), anti-PARP (9542, Cell Signaling Technology), anticaspase-3 (AAP-113, Stressgen Bioreagents), and HRP-conjugated anti-GAPDH (sc-5778, Santa Cruz).

In Vivo Efficacy Experiments. For in vivo efficacy experiments using the SJSA-1 tumor xenograft model, 5×10^6 SJSA-1 cancer cells with 50% Matrigel were injected sc on the dorsal side of SCID mice from Charles River, one tumor per mouse. When xenograft tumors reached a mean of ~100 mm^3 (70−130 mm^3), mice were randomized into groups of eight mice. Vehicle control (10% PEG400/3% Cremophor/87% PBS) was administered orally (po) once per day for 14 days. Compound **9** was administered orally once per day for 14 days at 10, 30, and 100 mg/kg. Tumor sizes and animal weights were measured three times per week. Data are represented as mean tumor volumes. Tumor volume (mm^3) = $(AB^2)/2$ where A and B are the tumor length and width (in mm), respectively. Statistical analyses were done using two-way ANOVA and unpaired two-tailed t test, using Prism (version 4.0, GraphPad). $P < 0.05$ was considered statistically significant.

For in vivo efficacy studies using the RS4;11 tumor xenograft model, the same protocol was used with the following modifications: RS4;11 tumor cells were used; dose schedule of 100 and 200 mg/kg.

AUTHOR INFORMATION

Corresponding Author

*Telephone: 734-615-0362. Fax: 734-647-9647. E-mail: shaomeng@umich.edu.

Author Contributions

[§]Y.Z., S.Y., and W.S. provided equal contributions.

Notes

The authors declare the following competing financial interest(s): Dr. Shaomeng Wang is an inventor on the compounds described in this study. The technology has been licensed by Ascenta and Sanofi for clinical development, and Dr. Shaomeng Wang receives royalty from the licensing. Dr. Wang is also a consultant for Ascenta.

ACKNOWLEDGMENTS

We are grateful for financial support from the National Cancer Institute, National Institutes of Health (Grants R01CA121279, P50CA06956, and P50CA097248), the University of Michigan Cancer Center (Core Grant P30CA046592), Ascenta Therapeutics, Inc., and Sanofi S.A.

ABBREVIATIONS USED

AUC, area under the curve; CAN, ceric ammonium nitrate; C_{max}, the maximum compound concentration from oral dosing; Cl, clearance; CYP, cytochrome P450; CH_2Cl_2, dichloromethane; EtOAc, ethyl acetate; H_2O, water; LC/MS, liquid chromatography−mass spectrometry; MDM2, murine double minute 2; MeCN, acetonitrile; NaOH, sodium hydroxide; PD, pharmacodynamics; PK, pharmacokinetics; po, oral administration; qD, once a day dosing; SCID, severe combined immunodeficient; $T_{1/2}$, half-life; TFA, trifluoroacetic acid; T_{max}, the time at which C_{max} is reached

REFERENCES

(1) Levine, A. J. p53, the cellular gatekeeper for growth and division. *Cell* **1997**, *88*, 323−331.

(2) El-Deiry, W. S. Regulation of p53 downstream genes. *Semin. Cancer Biol.* **1998**, *8*, 345−357.

(3) Vogelstein, B.; Lane, D.; Levine, A. J. Surfing the p53 network. *Nature* **2000**, *408*, 307−310.

(4) Hainaut, P.; Hollstein, M. p53 and human cancer: the first ten thousand mutations. *Adv. Cancer Res.* **2000**, *77*, 81−137.

(5) Wu, X.; Bayle, J. H.; Olson, D.; Levine, A. J. The p53-mdm2 autoregulatory feedback loop. *Genes Dev.* **1993**, *7*, 1126−1132.

(6) Kussie, P. H.; Gorina, S.; Marechal, V.; Elenbaas, B.; Moreau, J.; Levine, A. J.; Pavletich, N. P. Structure of the MDM2 oncoprotein bound to the p53 tumor suppressor transactivation domain. *Science* **1996**, *274*, 948−953.

(7) Vassilev, L. T.; Vu, B. T.; Graves, B.; Carvajal, D.; Podlaski, F.; Filipovic, Z.; Kong, N.; Kammlott, U.; Lukacs, C.; Klein, C.; Fotouhi, N.; Liu, E. A. In vivo activation of the p53 pathway by small-molecule antagonists of MDM2. *Science* **2004**, *303*, 844−848.

(8) Shangary, S.; Qin, D.; McEachern, D.; Liu, M.; Miller, R. S.; Qiu, S.; Nikolovska-Coleska, Z.; Ding, K.; Wang, G.; Chen, J.; Bernard, D.; Zhang, J.; Lu, Y.; Gu, Q.; Shah, R. B.; Pienta, K. J.; Ling, X.; Kang, S.; Guo, M.; Sun, Y.; Yang, D.; Wang, S. Temporal activation of p53 by a specific MDM2 inhibitor is selectively toxic to tumors and leads to complete tumor growth inhibition. *Proc. Natl. Acad. Sci. U.S.A.* **2008**, *105*, 3933−3938.

(9) Vassilev, L. T. p53 activation by small molecules: application in oncology. *J. Med. Chem.* **2005**, *48*, 4491−4499.

(10) Shangary, S.; Wang, S. Targeting the MDM2-p53 interaction for cancer therapy. *Clin. Cancer Res.* **2008**, *14*, 5318−5324.

(11) Ding, K.; Lu, Y.; Nikolovska-Coleska, Z.; Qiu, S.; Ding, Y.; Gao, W.; Stuckey, J.; Krajewski, K.; Roller, P. P.; Tomita, Y.; Parrish, D. A.; Deschamps, J. R.; Wang, S. Structure-based design of potent non-peptide MDM2 inhibitors. *J. Am. Chem. Soc.* **2005**, *127*, 10130−10131.

(12) Ding, K.; Lu, Y.; Nikolovska-Coleska, Z.; Wang, G.; Qiu, S.; Shangary, S.; Gao, W.; Qin, D.; Stuckey, J.; Krajewski, K.; Roller, P. P.; Wang, S. Structure-based design of spiro-oxindoles as potent, specific small-molecule inhibitors of the MDM2-p53 interaction. *J. Med. Chem.* **2006**, *49*, 3432−3435.

(13) Yu, S.; Qin, D.; Shangary, S.; Chen, J.; Wang, G.; Ding, K.; McEachern, D.; Qiu, S.; Nikolovska-Coleska, Z.; Miller, R.; Kang, S.; Yang, D.; Wang, S. Potent and orally active small-molecule inhibitors of the MDM2-p53 interaction. *J. Med. Chem.* **2009**, *52*, 7970−7973.

(14) Rew, Y.; Sun, D. Q.; De Turiso, F. G. L.; Bartberger, M. D.; Beck, H. P.; Canon, J.; Chen, A.; Chow, D.; Deignan, J.; Fox, B. M.; Gustin, D.; Huang, X.; Jiang, M.; Jiao, X. Y.; Jin, L. X.; Kayser, F.; Kopecky, D. J.; Li, Y. H.; Lo, M. C.; Long, A. M.; Michelsen, K.; Oliner, J. D.; Osgood, T.; Ragains, M.; Saiki, A. Y.; Schneider, S.; Toteva, M.; Yakowec, P.; Yan, X. L.; Ye, Q. P.; Yu, D. Y.; Zhao, X. N.; Zhou, J.; Medina, J. C.; Olson, S. H. Structure-based design of novel inhibitors of the MDM2-p53 interaction. *J. Med. Chem.* **2012**, *55*, 4936−4954.

(15) Allen, J. G.; Bourbeau, M. P.; Wohlhieter, G. E.; Bartberger, M. D.; Michelsen, K.; Hungate, R.; Gadwood, R. C.; Gaston, R. D.; Evans, B.; Mann, L. W.; Matison, M. E.; Schneider, S.; Huang, X.; Yu, D. Y.; Andrews, P. S.; Reichelt, A.; Long, A. M.; Yakowec, P.; Yang, E. Y.; Lee, T. A.; Oliner, J. D. Discovery and optimization of chromenotriazolopyrimidines as potent inhibitors of the mouse double minute 2-tumor protein 53 protein−protein interaction. *J. Med. Chem.* **2009**, *52*, 7044−7053.

(16) Czarna, A.; Beck, B.; Srivastava, S.; Popowicz, G. M.; Wolf, S.; Huang, Y. J.; Bista, M.; Holak, T. A.; Domling, A. Robust generation of lead compounds for protein−protein interactions by computational and MCR chemistry: p53/Hdm2 antagonists. *Angew. Chem., Int. Ed.* **2010**, *49*, 5352−5356.

(17) Gomez-Monterrey, I.; Bertamino, A.; Porta, A.; Carotenuto, A.; Musella, S.; Aquino, C.; Granata, I.; Sala, M.; Brancaccio, D.; Picone, D.; Ercole, C.; Stiuso, P.; Campiglia, P.; Grieco, P.; Ianelli, P.; Maresca, B.; Novellino, E. Identification of the spiro(oxindole-3,3′-thiazolidine)-

based derivatives as potential p53 activity modulators. *J. Med. Chem.* **2010**, *53*, 8319−8329.
(18) Hardcastle, I. R.; Liu, J. F.; Valeur, E.; Watson, A.; Ahmed, S. U.; Blackburn, T. J.; Bennaceur, K.; Clegg, W.; Drummond, C.; Endicott, J. A.; Golding, B. T.; Griffin, R. J.; Gruber, J.; Haggerty, K.; Harrington, R. W.; Hutton, C.; Kemp, S.; Lu, X. C.; McDonnell, J. M.; Newell, D. R.; Noble, M. E. M.; Payne, S. L.; Revill, C. H.; Riedinger, C.; Xu, Q.; Lunec, J. Isoindolinone inhibitors of the murine double minute 2 (MDM2)-p53 protein−protein interaction: structure−activity studies leading to improved potency. *J. Med. Chem.* **2011**, *54*, 1233−1243.
(19) Bold, G.; Furet, P.; Gessier, F.; Kallen, J.; Hergovich Lisztwan, J.; Masuya, K.; Vaupel, A. Tetra-Substituted Heteroaryl Compounds and Their Use as MDM2 and/or MDM4 Modulators. PCT Patent WO/2011/023677, 2011.
(20) Uoto, K.; Kawato, H.; Sugimoto, Y.; Naito, H.; Miyazaki, M.; Taniguchi, T.; Aonuma, M. Imidazothiazole Derivative Having 4,7-Diazaspiro[2.5]octane Ring Structure. PCT Patent WO/2009/151069, 2009.
(21) Zhao, Y.; Liu, L.; Sun, W.; Lu, J.; McEachern, D.; Li, X.; Yu, S.; Bernard, D.; Ochsenbein, P.; Ferey, V.; Carry, J.-C.; Deschamps, J. R.; Sun, D.; Wang, S. Diastereomeric spirooxindoles as highly potent and efficacious MDM2 inhibitors. *J. Am. Chem. Soc.* **2013**, *135*, 7223−7734.
(22) Garcia-Echeverria, C.; Chene, P.; Blommers, M. J. J.; Furet, P. Discovery of potent antagonists of the interaction between human double minute 2 and tumor suppressor p53. *J. Med. Chem.* **2000**, *43*, 3205−3208.
(23) Nikolovska-Coleska, Z.; Wang, R. X.; Fang, X. L.; Pan, H. G.; Tomita, Y.; Li, P.; Roller, P. P.; Krajewski, K.; Saito, N. G.; Stuckey, J. A.; Wang, S. M. Development and optimization of a binding assay for the XIAP BIR3 domain using fluorescence polarization. *Anal. Biochem.* **2004**, *332*, 261−273.